

Bis(phosphinimino)methanide Borohydride Complexes of the Rare-Earth Elements as Initiators for the Ring-Opening Polymerization of ϵ -Caprolactone: Combined Experimental and Computational Investigations

Jelena Jenter,^[a] Peter W. Roesky,^{*,[a]} Nouredine Ajellal,^[b] Sophie M. Guillaume,^{*,[b]} Nicolas Susperregui,^[c] and Laurent Maron^{*,[c]}

Abstract: Rare-earth-metal borohydrides are known to be efficient catalysts for the polymerization of apolar and polar monomers. The bis-borohydrides $[\{\text{CH}(\text{PPh}_2\text{NSiMe}_3)_2\}\text{La}(\text{BH}_4)_2(\text{THF})]$ and $[\{\text{CH}(\text{PPh}_2\text{NSiMe}_3)_2\}\text{Ln}(\text{BH}_4)_2]$ ($\text{Ln} = \text{Y}, \text{Lu}$) have been synthesized by two different synthetic routes. The lanthanum and the lutetium complexes were prepared from $[\text{Ln}(\text{BH}_4)_3(\text{THF})_3]$ and $\text{K}\{\text{CH}(\text{PPh}_2\text{NSiMe}_3)_2\}$, whereas the yttrium analogue was obtained from in situ prepared $[\{\text{CH}(\text{PPh}_2\text{NSiMe}_3)_2\}\text{YCl}_2]$ and NaBH_4 . All new compounds were char-

acterized by standard analytical/spectroscopic techniques, and the solid-state structures were established by single-crystal X-ray diffraction. The ring-opening polymerization (ROP) of ϵ -caprolactone initiated by $[\{\text{CH}(\text{PPh}_2\text{NSiMe}_3)_2\}\text{La}(\text{BH}_4)_2(\text{THF})]$ and $[\{\text{CH}(\text{PPh}_2\text{NSiMe}_3)_2\}\text{Ln}(\text{BH}_4)_2]$ ($\text{Ln} = \text{Y}, \text{Lu}$) was studied. At 0°C the

molar mass distributions determined were the narrowest values ($\bar{M}_w/\bar{M}_n = 1.06\text{--}1.11$) ever obtained for the ROP of ϵ -caprolactone initiated by rare-earth-metal borohydride species. DFT investigations of the reaction mechanism indicate that this type of complex reacts in an unprecedented manner with the first B–H activation being achieved within two steps. This particularity has been attributed to the metallic fragment based on the natural bond order analysis.

Keywords: boron • density functional calculations • lactones • rare earths • ring-opening polymerization

Introduction

Polyesters and -carbonates derived from heterocyclic monomers such as lactones, dilactones, and carbonates are being increasingly used for environmental applications as recyclable plastic substitutes or textile derivatives and more importantly as biomedical and pharmaceutical tools (diagnostic and therapeutic systems: controlled and sustained drug/gene delivery vehicles, tissue engineering, and tissue repair biomaterials).^[1–9] A wide range of initiating systems based on main group as well as d and f transition-metal derivatives have been designed and successfully evaluated in the ring-opening polymerization (ROP) of such heterocyclic monomers.^[5–13] Although rather “basic” complexes such as zinc bis-alkoxide species prepared in situ from ZnEt_2 and ROH are efficient in living processes,^[14–16] more sophisticated initiating systems involving metallocene and, more recently, post-metallocene ancillary ligands provide further control over the stereo-, regio-, and enantioselectivity, limiting side-reactions, and with high activity and productivity.^[15–19] In rare-earth chemistry, alkoxide and aryl oxide initiating sys-

[a] Dipl.-Chem. J. Jenter, Prof. Dr. P. W. Roesky
Institut für Anorganische Chemie
Karlsruher Institut für Technologie (KIT)
Engesserstr. 15, 76128 Karlsruhe (Germany)
Fax: (+49) 721-608-4845
E-mail: roesky@kit.edu

[b] N. Ajellal, Dr. S. M. Guillaume
Laboratoire Catalyse et Organométalliques
CNRS, Université de Rennes 1
Sciences Chimiques de Rennes (UMR 6226), Campus de Beaulieu
35042 Rennes Cedex (France)
Fax: (+33) 2-2323-6939
E-mail: sophie.guillaume@univ-rennes1.fr

[c] N. Susperregui, Prof. Dr. L. Maron
Université de Toulouse, INSA, UPS, CNRS-UMR5215, LPCNO
135 avenue de Rangueil, 31077 Toulouse (France)
Fax: (+33) 561-559-697
E-mail: laurent.maron@irsamc.ups-tlse.fr

Supporting information for this article is available on the WWW under <http://dx.doi.org/10.1002/chem.200903107>.

tems remain the most common and display high polymerization activity towards a wide variety of monomers.^[10–13, 19, 20] Of particular interest to this contribution is the ability of borohydride group 3 metal initiators to act as ROP catalysts for ϵ -caprolactone (CL), lactide, or carbonate.

The tris-borohydrides of the rare-earth elements $[\text{Ln}(\text{BH}_4)_3(\text{THF})_3]$ were initially prepared in the early 1950s by reaction of rare-earth-metal alkoxides with B_2H_6 .^[21] In the 1980s Mirsaidov and co-workers developed a more convenient approach starting from LnCl_3 ($\text{Ln} = \text{La, Ce, Pr, Nd, Sm}$) and NaBH_4 .^[22–24] Later on, greater value was given to these original species in the promotion of rare-earth borohydride organometallic chemistry^[25–28] and in their use as efficient catalysts for the (co)polymerization of ethylene,^[29–31] isoprene,^[31–35] styrene,^[34, 36] and some polar monomers such as lactide,^[37–42] ϵ -caprolactone,^[37–39, 43–52] trimethylene carbonate,^[52] and methyl methacrylate.^[53–57] Also, some rare-earth-metal borohydride derivatives such as metallocenes,^[31, 46] mono-cyclopentadienyl complexes,^[25, 33, 35–37] alkoxides,^[37, 40, 58] and guanidates^[40–42, 49, 55] have been used for different catalytic applications. Much of this interest in the tris-borohydrides arose from the many advantages that the BH_4^- ligand exhibits over other anionic ligands, especially over chloride, both in the organometallic and polymer domains. Although BH_4^- is isosteric with Cl^- , it is much more electron-donating,^[59] thereby allowing the isolation of otherwise unsaturated and inaccessible metallic species. Note, certain rare-earth compounds are more easily synthesized and isolated from borohydride precursors than the corresponding halide or alkoxide analogues, which rather lead to “ate,” aggregated, or bridged derivatives that are also less soluble. In addition, borohydride species exhibit some of the hydridic character of the valuable hydride homologues through one, two, or three $\text{Ln}(\mu\text{-H})\text{B}$ linkages.^[60–62] The BH_4^- ligand is also conveniently identified and monitored by ^1H and/or ^{11}B NMR as well as by IR spectroscopy. This provides an invaluable “handle” both for the characterization of reaction products as well as for in situ monitoring of experiments to identify intermediates and elucidate reaction mechanisms. With regard to the polymerization of polar monomers, the major benefit of the borohydride initiating species is that they provide direct access to the highly valuable α,ω -dihydroxytelechelic polyesters.^[38, 39, 44–50] This relies on the in situ reduction of the carbonyl group of the first inserted cyclic ester molecule (CL or lactide (LA)) by the BH_4^- function (see below).^[38, 44–52] Indeed, dihydroxy-terminally functionalized PCLs (HO-PCL-OH)^[44–50] or PLAs (HO-PLA-OH)^[38, 39] have been easily prepared without the inherent constraints associated with post-polymerization chemical modification, as fully evidenced by ^1H and ^{13}C NMR spectroscopy and MALDI-TOF MS analyses. Indirect support for the formation of dihydroxy-terminated polyesters was also provided by the successful chain-extension synthesis of AB_2 triblock copolymers, poly(caprolactone)-*b*-[poly(benzylglutamate)]₂ and poly(caprolactone)-*b*-[poly(methyl methacrylate)]₂^[54] or of poly(ester-urethane).^[39] The general polymerization process, especially the key step of the formation of the propa-

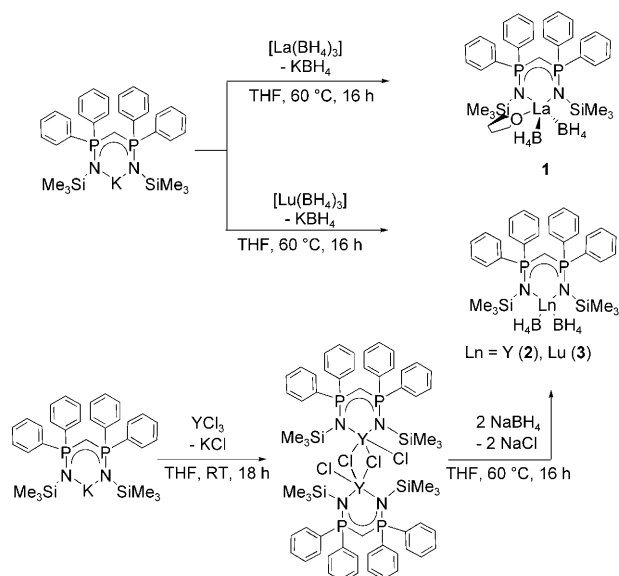
gating species as an aliphatic alkoxide with a terminal CH_2OBH_2 group, proceeds by a well-demonstrated, both experimentally and theoretically, and a well-accepted mechanism that is common to all borohydride initiating species.^[39, 43–48]

Recently, we introduced the bis(phosphinimino)methanide $\{\text{CH}(\text{PPh}_2\text{NSiMe}_3)_2\}^-$, which has been used previously by a number of research groups in main-group and transition-metal chemistry,^[63–66] into yttrium and lanthanide chemistry as a replacement for cyclopentadienyl.^[51, 67–75] In general the $\text{CH}_2(\text{PPh}_2\text{NSiMe}_3)_2$ ligand is very easily accessible. It can be made in a Staudinger reaction in a few hours without solvent from commercially available starting materials.^[76] In this context we showed that the chloride complexes $[\{\text{CH}(\text{PPh}_2\text{NSiMe}_3)_2\}\text{Ln}(\text{Cp}^*)\text{Cl}]$ ($\text{Ln} = \text{Y, Sm, Yb}$; $\text{Cp}^* = (\eta^5\text{-C}_5\text{Me}_5)$) combined in situ with 1 equiv of 2-propanol enables the living ROP of CL to polymers with controlled molecular features (end-groups, \bar{M}_n) and very narrow molar mass distributions.^[51]

In this contribution we report the use of this bis(phosphinimino)methanide ligand in the synthesis of novel rare-earth-metal bis-borohydride complexes and an evaluation of their efficacy as initiators for the ROP of CL. Furthermore, as a continuation of our recent efforts to gain an insight into the polymerization of polar monomers by group 3 borohydride derivatives,^[43, 53] we combined our experimental studies with DFT calculations. In particular, we investigated the influence of the bis(phosphinimino)methanide ligand on the energetics and competing pathways of the first step of the ROP, that is, the reaction between the rare-earth metal complex and the first monomer molecule, which leads to the active alkoxide species. Our initial work on the ROP of CL with the non-metallocene, the metallocene, and the post-metallocene lanthanide borohydride systems, modeled as $[\text{Eu}(\text{BH}_4)_3]$, $[(\text{Cp})_2\text{Eu}(\text{BH}_4)]$ ($\text{Cp} = (\eta^5\text{-C}_5\text{H}_5)$), and $[(\text{N}_2\text{NN}')\text{Eu}(\text{BH}_4)]$ ($\text{N}_2\text{NN}' = (2\text{-C}_5\text{H}_4\text{N})\text{CH}_2\text{N}(\text{CH}_2\text{CH}_2\text{NMe})_2$), respectively,^[43] included a comparison with the model hydride complex $[(\text{Cp})_2\text{Eu}(\text{H})]$ of Yasuda and co-workers for which experimental results have already been reported for the real system $[(\text{Cp}^*)_2\text{Sm}(\mu\text{-H})_2]$.^[77, 78] Although these computational results were in complete agreement with experimental findings for both the hydride and borohydride species, some differences between the hydride and borohydride, and more importantly between metallocene and non-metallocene borohydride precursors, were highlighted. The greater negative charge carried by the $\text{N}_2\text{NN}'$ ligand compared with $(\text{Cp})_2$ was shown to have a significant impact on the earlier step of the ROP in reducing the interaction between the reactive ligands (borohydride or alkoxide) and the metal center. Based on these preliminary findings, the bis(phosphinimino)methanide ligand was expected to play a significant role in the initial step of the ROP of CL.

Results and Discussion

Synthesis of the metal complexes: The desired bis(phosphin-imino)methanide rare-earth-metal bis-borohydrides solvated $[\{\text{CH}(\text{PPh}_2\text{NSiMe}_3)_2\}\text{La}(\text{BH}_4)_2(\text{THF})]$ (**1**) and unsolvated $[\{\text{CH}(\text{PPh}_2\text{NSiMe}_3)_2\}\text{Ln}(\text{BH}_4)_2]$ ($\text{Ln} = \text{Y}$ (**2**), Lu (**3**)) were obtained by two different synthetic routes. The first approach, which was used for the synthesis of compounds **1** and **3**, started from $[\text{Ln}(\text{BH}_4)_3(\text{THF})_3]$ and $\text{K}[\text{CH}(\text{PPh}_2\text{NSiMe}_3)_2]$.^[79] The salt metathesis reactions performed in THF at elevated temperature resulted in the target compounds in good yields (Scheme 1).^[80] In contrast,



Scheme 1.

the yttrium complex **2** was obtained in a two-step one-pot procedure. First, $\text{K}[\text{CH}(\text{PPh}_2\text{NSiMe}_3)_2]$ was treated with anhydrous yttrium trichloride to give the known dimeric complex $[\{\text{CH}(\text{PPh}_2\text{NSiMe}_3)_2\}\text{YCl}_2]_2$.^[67] In situ prepared $[\{\text{CH}(\text{PPh}_2\text{NSiMe}_3)_2\}\text{YCl}_2]_2$ was then treated with NaBH_4 to give compound **2** in good yield (Scheme 1).^[80] Because the starting material $[\text{Ln}(\text{BH}_4)_3(\text{THF})_3]$ for the syntheses of **1** and **3** was obtained from LnCl_3 and NaBH_4 , both synthetic routes are roughly equally time consuming.

The new complexes **1–3** were characterized by standard analytical/spectroscopic techniques and the solid-state structures were established by single-crystal X-ray diffraction. To have the possibility of characterizing all the new compounds by NMR spectroscopy, only diamagnetic rare-earth metal ions were used. The ^1H NMR spectra of **1–3** show signals characteristic of the two different substituents. The BH_4^- anions are observed as broad signals at $\delta = 1.02\text{--}1.64$ (**1**), $1.70\text{--}2.10$ (**2**), and $1.45\text{--}2.08$ ppm (**3**). More characteristic are the ^{11}B NMR signals of these groups, which are resolved into a quintet for compounds **1** and **2** ($J_{\text{BH}} = 83$ (**1**) and 108 Hz (**2**)), whereas for compound **3** only a broad signal is seen ($\delta = -22.4$ (**1**), -24.7 (**2**), and -25.8 ppm (**3**)). For the

$\{\text{CH}(\text{PPh}_2\text{NSiMe}_3)_2\}^-$ ligands, one singlet typical of the SiMe_3 groups ($\delta = 0.22$ (**1**), 0.19 (**2**), and 0.35 ppm (**3**)) and a triplet for the PCHP groups ($\delta = 2.02$ (**1**), 1.94 (**2**), and 1.83 ppm (**3**)) are observed. In the $^{31}\text{P}\{^1\text{H}\}$ NMR spectrum, one signal characteristic of the $\{\text{CH}(\text{PPh}_2\text{NSiMe}_3)_2\}^-$ ligand is observed ($\delta = 15.6$ (**1**), 17.8 (**2**), and 20.9 ppm (**3**)). For the yttrium compound **2**, this signal is split into a doublet as a result of $^2J(\text{P}, \text{Y})$ coupling. In the EI-MS spectra, a molecular peak is observed as expected for each compound. In the IR spectra of compounds **1–3**, two characteristic peaks for each complex at 2210 and 2424 cm^{-1} (**1**), 2216 and 2486 cm^{-1} (**2**), and 2225 and 2495 cm^{-1} (**3**) are observed, which can be assigned to a terminal tridentate $\text{Ln}(\eta^3\text{-H}_3\text{B-H})$ unit.^[60–62]

Compound **1** crystallizes in the monoclinic space group $P2_1/n$ with four molecules of **1** and eight molecules of THF in the unit cell (Figure 1). The coordination polyhedron of

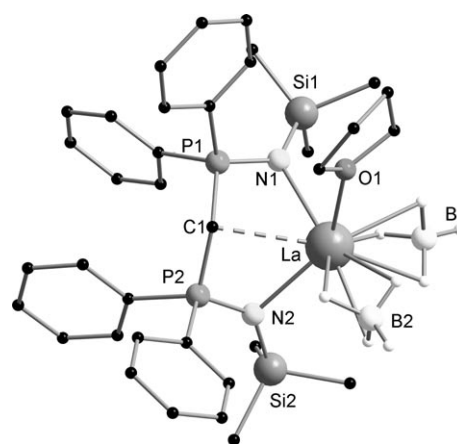


Figure 1. Solid-state structure of **1** showing the atomic labeling scheme and omitting hydrogen atoms, except for the freely refined B–H atoms. Selected bond lengths [Å] and angles [°]: La–N1 2.552(3), La–N2 2.556(3), La–O1 2.540(3), La–B1 2.706(5), La–B2 2.727(6), La–C1 2.789(3), N1–P1 1.598(3), N1–Si1 1.734(3), N2–P2 1.599(3), N2–Si2 1.728(3), C1–P2 1.745(3), C1–P1 1.748(3); N1–La–N2 89.36(10), N1–La–O1 80.59(10), N2–La–O1 142.82(9), N1–La–B1 93.3(2), N2–La–B1 111.38(14), N1–La–B2 160.19(15), N2–La–B2 98.3(2), N1–La–C1 61.34(10), N2–La–C1 60.51(9), O1–La–B1 104.90(14), O1–La–B2 82.3(2), B1–La–B2 100.8(2), O1–La–C1 83.55(10), B1–La–C1 152.1(2), B2–La–C1 106.8(2), P1–C1–P2 125.5(2).

complex **1** is formed by two BH_4^- anions, one molecule of THF, and the $\{\text{CH}(\text{PPh}_2\text{NSiMe}_3)_2\}^-$ ligand. The hydrogen atoms of the BH_4^- groups, which were freely refined, show an η^3 coordination. This coordination mode is typical for Ln-BH_4 compounds.^[24,26,27,40,60–62] If the BH_4^- group is considered as monodentate and the $\{\text{CH}(\text{PPh}_2\text{NSiMe}_3)_2\}^-$ ligand as tridentate, the structures present a six-fold coordination sphere of ligands around the metal atom and adopt a distorted octahedral coordination polyhedron (e.g., B1–La–B2 $100.8(2)^\circ$). The $\{\text{CH}(\text{PPh}_2\text{NSiMe}_3)_2\}^-$ ligand forms a six-membered metallacycle (N1–P1–C1–P2–N2–La) by chelation of the two trimethylsilylimine groups to the lanthanum atom (La–N1 2.552(3) Å and La–N2 2.556(3) Å). The ring adopts a typical twist-boat conformation in which the central

carbon atom and the lanthanum atom are displaced from the N_2P_2 least-squares plane.^[66] As expected, a weak interaction between the central carbon atom (C1) and the lanthanum atom is observed (La–C1 2.789(3) Å). This distance is longer than observed for normal La–C bonds.^[81]

Compounds **2** and **3** are isostructural. Both compounds crystallize in the monoclinic space group $P2_1/n$ with four molecules of each complex in the unit cell (Figure 2). As a

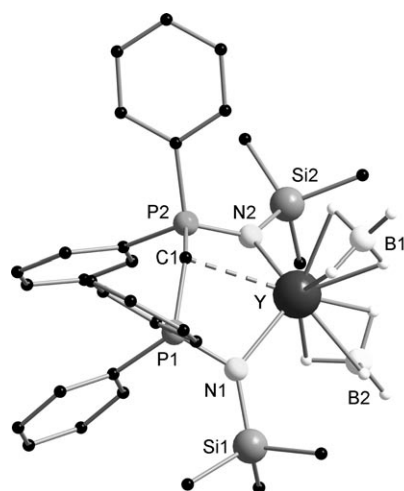


Figure 2. Solid-state structure of **2** showing the atomic labeling scheme and omitting hydrogen atoms, except for the freely refined B–H atoms. Selected bond lengths [Å] and angles [°] (also given for isostructural **3**): N1–Y 2.297(2), N2–Y 2.328(2), Y–C1 2.651(3), B1–Y 2.496(4), B2–Y 2.500(4), N1–P1 1.611(2), N1–Si1 1.746(2), N2–P2 1.605(2), N2–Si2 1.742(2), C1–P2 1.736(3), C1–P1 1.746(3); N1–Y–N2 113.79(8), N1–Y–B1 116.61(13), N2–Y–B1 116.71(12), N1–Y–B2 96.50(12), N2–Y–B2 98.22(12), N1–Y–C1 65.98(8), N2–Y–C1 65.41(8), B1–Y–B2 111.2(2), B1–Y–C1 104.13(15), B2–Y–C1 144.66(13), P1–C1–P2 133.42(2). **3**: Lu–N1 2.256(3), Lu–N2 2.290(3), Lu–B1 2.436(5), Lu–B2 2.449(5), Lu–C1 2.620(3), N1–P1 1.607(3), N1–Si1 1.748(3), N2–P2 1.601(3), N2–Si2 1.745(3), C1–P2 1.743(3), C1–P1 1.748(3); N1–Lu–N2 115.24(10), N1–Lu–B1 115.75(14), N2–Lu–B1 116.76(14), N1–Lu–B2 96.80(14), N2–Lu–B2 97.71(14), N1–Lu–C1 66.95(10), N2–Lu–C1 66.42(9), B1–Lu–B2 110.7(2), B1–Lu–C1 103.3(2), B2–Lu–C1 146.0(2), P1–C1–P2 132.3(2).

result of the smaller ion radius of the central metal atom, there is no solvent molecule in the coordination sphere. The coordination polyhedra of complexes **2** and **3** are therefore formed by two BH_4^- anions and the $\{CH(PPh_2NSiMe_3)_2\}^-$ ligand only. As observed for compound **1**, the hydrogen atoms of the BH_4^- groups, which were freely refined, show an η^3 coordination. Similar to compound **1**, six-membered metallacycles (N1–P1–C1–P2–N2–Ln), which adopt a twist-boat conformation, are formed by the $\{CH(PPh_2NSiMe_3)_2\}^-$ ligands and the metal atoms with Ln–N bond distances of N1–Y 2.297(2) Å and N2–Y 2.328(2) Å for **2** and Lu–N1 2.256(3) Å and Lu–N2 2.290(3) Å for **3**. The distances between the central carbon atom (C1) and the lanthanide atom (2.651(3) Å (**2**) and 2.620(3) Å (**3**)) are longer than usual Ln–C distances, however, the folding of the six-membered ring towards the lanthanide atom is caused by a weak interaction. The twist-boat conformation of the six-membered metallacycle has been observed in all the bis(phosphinimino)methanide lanthanide compounds that we have synthesized so far.^[82] We have previously shown that the weak Ln–C interaction depends not only on the size of the lanthanide atom and the coordination sphere, but also significantly on crystal-packing effects.^[68,83]

Ring-opening polymerization of ϵ -caprolactone: The ring-opening polymerization of CL initiated by either the bis-(phosphinimino)methanide lanthanum, yttrium, or lutetium bis-borohydride complexes **1–3** proceeded smoothly at room temperature in THF (Table 1). In all the experiments, the monomer conversion was nearly quantitative and the polymer was recovered in yields of at least 90% along with a minor fraction of residual products. All three metallic compounds allowed control of the ROP of CL in terms of molar mass and molar mass distribution with monomer-to-initiator ratios of up to 300. Under such experimental conditions, polymers with \bar{M}_n values of up to 22400 g mol^{−1} could be obtained. Molar masses measured by size exclusion chromatography (SEC) were in good agreement with the calculated

Table 1. Polymerization of CL initiated by **1–3** at 20 °C.^[a]

Entry	[M]	[CL] ₀ /[M] ₀	Solvent	Reaction temperature [°C]	Reaction time ^[b] [min]	Conv. ^[c] [%]	$\bar{M}_{n,theo}$ ^[d] [10 ³ g mol ^{−1}]	$\bar{M}_{n,SEC}$ ^[e] [10 ³ g mol ^{−1}]	\bar{M}_w/\bar{M}_n ^[f]	TOF [mol _{CL} mol _{initiator} ^{−1} h ^{−1}]
1	La	50	THF	20	2	100	2.8	2.2	1.16	1500
2	La	300	THF	20	1	98	16.8	13.4	1.38	17640
3	La	300	THF	0	20	95	16.2	15.7	1.11	855
4	La	220	Tol	20	0.5	95	11.9	12.9	1.47	25080
5	Y	50	THF	20	2	100	2.8	2.6	1.18	1500
6	Y	100	THF	20	5	100	5.7	5.6	1.40	1200
7	Y	250	THF	20	100	100	14.3	15.1	1.45	150
8	Y	300	THF	20	1	92	16.2	15.7	1.49	16560
9	Y	250	THF	0	30	98	14.0	14.3	1.09	490
10	Y	250	Tol	20	300	99	14.1	22.4	1.84	50
11	Lu	300	THF	20	1	98	16.8	15.3	1.35	17640
12	Lu	300	THF	0	20	96	16.4	15.8	1.06	864
13	Lu	300	Tol	20	0.5	95	16.2	14.2	1.48	34200

[a] Results are representative of at least two experiments. [b] Reaction times were not necessarily optimized. [c] Monomer conversions were determined by ¹H NMR spectroscopy. [d] Theoretical molar masses were calculated from $[CL]_0/2[M]_0 \times \text{monomer conversion} \times M_{CL}$ with $M_{CL} = 114 \text{ g mol}^{-1}$. [e] Experimental molar masses were determined by SEC versus polystyrene standards and corrected by a factor of 0.56.^[44] [f] Molar mass distributions were calculated from SEC traces.

data and increased proportionally to the monomer feed ratio. The molar mass distributions for experiments performed at ambient temperature, although within a reasonable range, are larger than those (typically 1.2–1.3) recorded with the pendant tris-borohydride $[\text{Ln}(\text{BH}_4)_3(\text{THF})_3]$ ($\text{Ln} = \text{La}, \text{Nd}, \text{Sm}$) or mono-borohydride $[(\eta^5\text{-C}_5\text{Me}_5)_2\text{Sm}(\text{BH}_4)(\text{THF})]$ complexes.^[44–47] This reflects the occurrence of side-reactions that are typical in the ROP of cyclic esters, for example, transfer and transesterification (bimolecular reshuffling or intramolecular backbiting) reactions.^[84,85] The moderate molar mass distributions can also be attributed to a rate of propagation that is faster than the rate of initiation. With respect to the values of \bar{M}_w/\bar{M}_n , the ROP appears to be slightly less controlled in toluene (entries 4, 10, and 13), whereas lowering of the reaction temperature resulted in significantly improved control and activity of the catalyst (entries 2 vs. 3, 8 vs. 9, and 11 vs. 12). Indeed, at 0°C, the molar mass distributions show the narrowest values ($\bar{M}_w/\bar{M}_n = 1.06\text{--}1.11$) ever obtained for the ROP of CL initiated by rare-earth-metal borohydride species.^[37,39,44–50] This strongly suggests that at 0°C the propagation rate is lower (and thereby the initiation rate is relatively not as slow) than that at 23°C and that the ROP at 23°C is too fast thereby leading to some side-reactions within the experimental reaction time, a phenomenon that can be considerably limited by lowering the reaction temperature. As illustrated by the TOF values reported in Table 1, all three catalysts are highly active. In comparison with the activities of related rare-earth-metal borohydrides in the ROP of CL, which typically do not exceed $\text{TOF} = 1810 \text{ mol}_{\text{CL}} \text{ mol}_{\text{initiator}}^{-1} \text{ h}^{-1}$,^[39,48–50] the extremely high activities of up to $\text{TOF} = 34200 \text{ mol}_{\text{CL}} \text{ mol}_{\text{initiator}}^{-1} \text{ h}^{-1}$ recorded in this work (entries 2, 4, 8, 11, and 13) are in the same range as those obtained with the bridging mono-borohydride diamino bis(phenoxide) samarium derivatives ($\text{TOF} = 29700 \text{ mol}_{\text{CL}} \text{ mol}_{\text{initiator}}^{-1} \text{ h}^{-1}$).^[37] Thus, the ancillary ligand in this latter case,^[37] as well as in this work, most likely significantly and positively influences the control of the ROP of CL. No significant difference relating to the ion radius of the metal was observed because all three metallic complexes exhibited similar activity both at 20°C (entries 2, 8, and 11) and at 0°C (entry 3, 9, and 12) for a monomer-to-initiator ratio of 300–250 within a similar reaction time (1 and 20–30 min, respectively).

For all the initiators **1–3**, NMR data of all the polymers recovered after precipitation in methanol showed the formation of α,ω -dihydroxytelechelic PCL, HO-PCL-OH (see the Supporting Information). This is evidenced by the observation in the ^1H NMR spectra of the typical triplet at $\delta = 3.82$ ppm corresponding to the methylene group at the α position with respect to the terminal hydroxy function alongside the main polymer chain signals. Similarly, the ^{13}C NMR spectra exhibits signals at $\delta = 62.1$ and 32.4 ppm for the HOCH_2CH_2 methylene groups, respectively, in the polymer chain end. No other chain end signal was detected, which supports the formation of dihydroxy-functionalized PCL, HO-PCL-OH. This supports the oxygen–acyl bond cleavage of the cyclic ester as expected.^[44–47]

Computational investigations: Based on our previous experience^[43,53] and to gain more insight into the reaction mechanism, a DFT study of the reaction of the yttrium complex **2** with CL, that is, the initiation step leading to the active species, was carried out. To save some computational time, the ligand was simplified; the phenyl rings were replaced by methyl groups and the SiMe_3 groups by SiH_3 . Such a modeling strategy, which does not influence the reactivity of the ligand, has already been successfully applied.^[43] The calculated free-energy profile for the reaction of $[\{\text{CH}(\text{PMe}_2\text{NSiH}_3)_2\}\text{Y}(\text{BH}_4)_2]$ with CL was determined by this approach (Figure 3).

The calculated reaction mechanism depicted in pathway a) of Scheme 2 and Figure 3 is very similar to the one previously proposed for the borohydride complexes

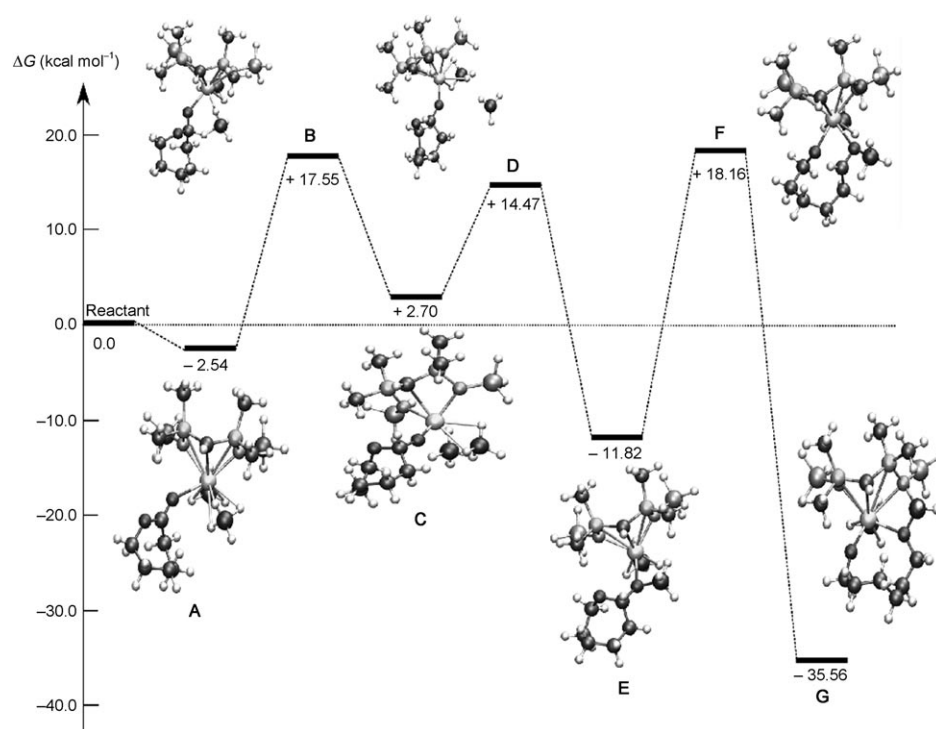
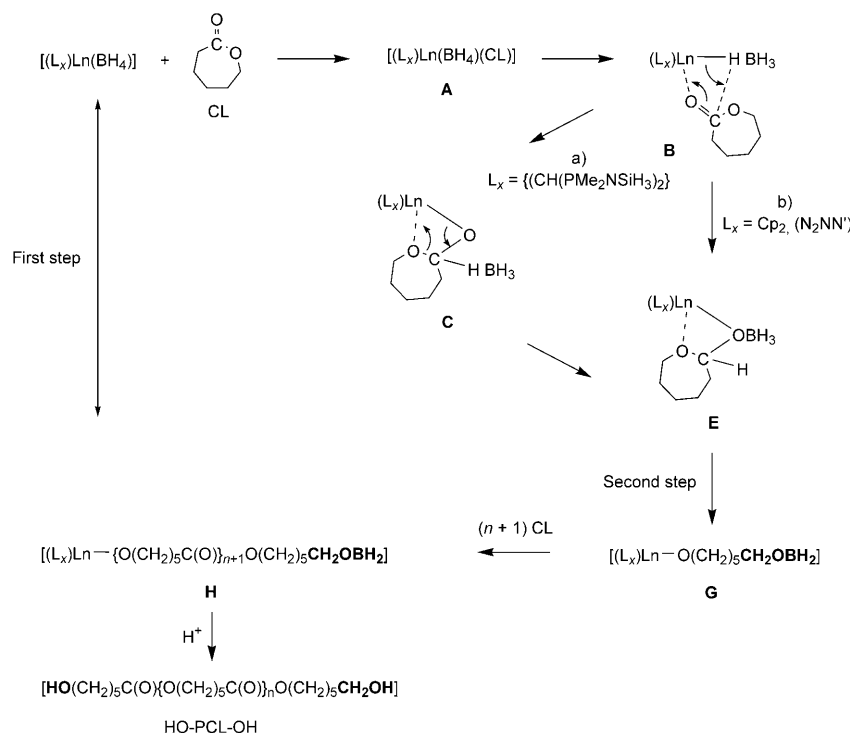


Figure 3. Calculated free-energy profile for the reaction of ϵ -caprolactone with $[\{\text{CH}(\text{PMe}_2\text{NSiH}_3)_2\}\text{Y}(\text{BH}_4)_2]$.



Scheme 2. Proposed general mechanism for the polymerization of ϵ -caprolactone initiated by $[(L)_xLn(BH_4)]$ ($L_x = (Cp)_2, (N_2NN')$ ^[43] and $[CH(PMe_2NSiH_3)_2]$).

$[(Cp)_2Eu(BH_4)]$ and $[(N_2NN')Eu(BH_4)]$ (Scheme 2, pathway b)^[43] in that it proceeds in two steps, a hydride transfer from the rare-earth complex to the carbonyl carbon atom of the CL (Scheme 2, Figure 3: reactant **E**) followed by the ring-opening of the cyclic ester by oxygen–acyl bond cleavage (Scheme 2, Figure 3: **E**→**G**), which implies two successive B–H activations leading to the formation of a terminal CH_2OBH_2 (**G**; Scheme 2a, Figure 3). As demonstrated before both experimentally^[44–48] and theoretically,^[43] the formation of the alkoxyborane group in **G** arises from the reduction of the adjacent carbonyl group of the lactone by BH_3 (Scheme 2, second step). The propagation step (Scheme 2, **G**→**H**) involves the coordination–insertion polymerization of further CL molecules through the $Ln-O$ bond, which gives rise to the active polymer species **H**. Finally, quenching and deactivation of the reaction results in the hydrolysis of the $Ln-O$ and CH_2O-BH_2 bonds of **H**, which generates a hydroxy end-group at each chain end, that is, the formation of α,ω -dihydroxytelechelic PCL, HO-PCL-OH, in agreement with the experimental observations reported above (Scheme 2, HO-PCL-OH; note that formally speaking, the final polymer should be referred to as H-PCL-O(CH_2)₆OH because H and O(CH_2)₆OH cap the PCL chains.). The reaction is predicted to be both kinetically and thermodynamically accessible.

The calculations performed in this work involving the bis-(phosphinimino)methanide ligand show one main difference with the reaction mechanism involving either the metallocene $(Cp)_2$ or non-metallocene (N_2NN') ancillary ligands in

that the formation of the borate ($C(O)HBH_3$) **E** is achieved in two steps (Scheme 2, pathway a, Figure 3: **A**→**C** and **C**→**E**) rather than in a straightforward unique step (Scheme 2, pathway b: **A**→**E**). In the first step, one hydride of the BH_4^- ligand classically attacks the ketonic carbon of the CL (Scheme 2, Figure 3: **A**→**C**). This process is rather low in energy (activation barrier of $20.1 \text{ kcal mol}^{-1}$ with respect to the CL adduct **A**). This barrier is similar to that calculated for the $[(Cp)_2Eu(BH_4)]$ complex ($23.65 \text{ kcal mol}^{-1}$).^[43] As opposed to the reaction pathway with $(Cp)_2$ or (N_2NN') derivatives in which BH_3 is trapped by the oxygen, this nucleophilic attack does not lead to the release of BH_3 , which in this case remains coordinated to the hydride (Scheme 2, Figure 3: **C**). The formation of such an adduct **C** is predicted to be

slightly endergonic ($+2.7 \text{ kcal mol}^{-1}$), which indicates a strong adduct (Figure 3). This was not expected as the formation of this adduct requires the cleavage of a strong electrostatic interaction between the borohydride ligand and the metal center. However, one significant difference to our previous study^[86] is that this investigation deals with bis-borohydride complexes as opposed to single-site mono-borohydride species. The additional BH_4^- ligand modifies the reactivity by inducing an interaction between BH_3 and the other BH_4^- ligand in **C**, as is indeed clearly observed in silico. The calculations are supported by some recently reported experimental results in which a redox reaction of a $Ln-BH_4$ complex gave a BH_3 molecule as a byproduct. The latter was trapped in the coordination sphere of the lanthanide complex.^[86]

Natural bonding orbital analysis (NBO) indicates that the charge of the metal center in **C** is not as high as in the metallocene complex ($+1.25$ in $[CH(PMe_2NSiH_3)_2]Y(BH_4)_2]$ vs. $+2.15$ in $[(Cp)_2Eu(BH_4)]$ and $[N_2NN'Eu(BH_4)]$) such that the loss of the electrostatic interaction is less dramatic in this complex than in the metallocene. At the same time, the charge on the boron atom is diminishing and the charge on the ketonic oxygen is increasing (up to -0.81). These charge distributions are definitely a signature of the bis(phosphinimino)methanide ligand being a rather good donor.

In the second step (Scheme 2–pathway a, Figure 3: **C**→**E**), BH_3 is trapped by the oxygen atom of the ketone, which leads to the formation of the borate **E**. The barrier for this process ($11.7 \text{ kcal mol}^{-1}$) is lower than for the first step

(20.1 kcal mol⁻¹) but is significant enough to define an overall double hump process (Figure 3: **A**→**E**). The formation of the borate complex (OBH₃) **E** is predicted to be thermodynamically favorable by 11.8 kcal mol⁻¹. Note that the charge on the metal fragment has increased to +1.53 in the latter complex, which further indicates the versatility of the bis(phosphinimino)methanide ligand. However, this borate complex **E** is less stable than that obtained with the metallocene [(Cp)₂SmBH₄] in which the charge at the metal center is higher (around +2.20).^[86] Thus, this two-step pathway leading to intermediate **E** results from a combined favorable effect of the simultaneous presence of two BH₄⁻ groups along with the more favorable electronic environment provided by the enveloping bis(phosphinimino)methanide ligand. During the trapping process, the second BH₄⁻ ligand remains bonded to the metal center in a η^3 fashion. This clearly indicates that the BH₃ ligand is only slightly interacting with the BH₄⁻ ligand in complex **C** in a donor–acceptor manner (interaction between the hydride BH₄⁻ and the empty p orbital of BH₃).

The ring-opening of the monomer thus occurs in the last step (Scheme 2, Figure 3: **E**→**G**), that is, in the borate complex **E**, by a second B–H activation process. Throughout the process, the second BH₄ ligand remains bonded to the metal center. This final step is thermodynamically favored making the overall reaction thermodynamically possible, very similar to those already calculated, and is classical for the polymerization of lactones catalyzed by borohydride complexes.^[43,53] The activation barrier is predicted to be 30.0 kcal mol⁻¹ with respect to the borate complex **E** (19.8 kcal mol⁻¹ with respect to the entrance channel **A**). The calculated most favorable complex formed from the reaction of [[CH(PMe₂NSiH₃)₂]Y(BH₄)₂] with CL, the alkoxide–borate **G** (with an OBH₂ terminus, Figure 3), thus exactly matches the experimentally postulated active species **G** (Scheme 2). As reported for the [(N₂NN')Eu(BH₄)] case, the borate is still formed in the transition state **F**, but it interacts with the metal center through the oxygen atom rather than through the hydrogen atoms. This is once again associated with the charge of the {CH(PMe₂NSiH₃)₂}⁻ ligand, which reduces the charge of the metal center. However, the versatility of the ligand, already underlined, allows an increase in the charge of the metal center such that the formation of **G** is highly exergonic. Thus, the {CH(PMe₂NSiH₃)₂}⁻ ligand is an excellent ligand for CL polymerization and its versatility may allow polymerization of MMA as does the (N₂NN') ligand.

Conclusion

The rare-earth metal bis-borohydrides [[CH(PPh₂NSiMe₃)₂]-Ln(BH₄)₂(THF)] and [[CH(PPh₂NSiMe₃)₂Ln(BH₄)₂] (Ln = Y, Lu) have been synthesized by two different synthetic routes. Complexes **1** and **3** were prepared from [Ln(BH₄)₃-(THF)₃] and K[CH(PPh₂NSiMe₃)₂], whereas the yttrium analogue **2** was obtained from in situ prepared

[[CH(PPh₂NSiMe₃)₂]YCl₂]₂ and NaBH₄. All the new compounds were characterized by standard analytical/spectroscopic techniques and the solid-state structures were established by single-crystal X-ray diffraction. The hydrogen atoms of the BH₄⁻ groups, which were freely refined, show η^3 coordination.

Complexes **1–3** successfully allowed the ring-opening polymerization of CL with nearly quantitative monomer conversion. The molar mass distributions for experiments performed at ambient temperature are larger than those recorded with the pendant tris-borohydride [Ln(BH₄)₃(THF)₃] (Ln = La, Nd, Sm) or mono-borohydride [[η^5 -C₅Me₅)₂Sm-(BH₄)(THF)] complexes, which is indicative of the occurrence of side-reactions. In contrast, at 0 °C, the molar mass distributions show the narrowest values (\bar{M}_w/\bar{M}_n = 1.06–1.11) ever obtained for the ROP of CL initiated by a rare-earth-metal borohydride species. These results thereby highlight the good control of the polymerization in terms of molar mass and limited side-reactions, most likely a result of the enveloping bis(phosphinimino)methanide ligand.

DFT investigations revealed a rather unique mechanism for the reaction between the bis-borohydride bis(phosphinimino)methanide complexes [[CH(PMe₂NSiH₃)₂]Y(BH₄)₂] and the first added CL molecule. Indeed, the first B–H activation of BH₄⁻ is achieved in two distinct unprecedented steps: nucleophilic attack of one hydride on the carbon atom of the ketone with decoordination of BH₄⁻ from the metal center and then trapping of BH₃ by the oxygen atom of the ketone. This contrasts with the single step required with mono-borohydride complexes. NBO analysis reveals that this difference in mechanism can be attributed to the metallic fragment. The positive effect of the simultaneous presence of two BH₄⁻ groups along with the greater electron-donating nature of the enveloping bis(phosphinimino)methanide ligand is thus the reason for the differences between the borohydrides studied in this work compared with previous studied ones.^[43] The subsequent ring-opening is classical of borohydride complexes and is achieved by a second B–H activation. The reaction was calculated to be kinetically facile and thermodynamically favorable, in agreement with experimental data.

Experimental Section

Materials: All manipulations of air-sensitive materials were performed with the rigorous exclusion of oxygen and moisture in flame-dried Schlenk-type glassware either on a dual manifold Schlenk line, interfaced to a high vacuum (10⁻³ torr) line, or in an argon-filled MBraun or Jacomex glove box. THF was distilled under nitrogen from potassium benzophenone ketyl prior to use. Hydrocarbon solvents (toluene and *n*-pentane) were dried by using an MBraun solvent purification system (SPS-800). All solvents for vacuum-line manipulations were stored in vacuo over LiAlH₄ in resealable flasks. ϵ -Caprolactone (ϵ -CL, Lancaster) was successively dried over CaH₂ (at least 1 week) and then over 4,4'-methylenebis(phenyl isocyanate). LnCl₃,^[87] K[CH(PPh₂NSiMe₃)₂],^[79] [Ln(BH₄)₃-(THF)₃],^[25] and [[CH(PPh₂NSiMe₃)₂]YCl₂]₂^[67] were prepared according to literature procedures. Deuterated solvents were obtained from Aldrich (99 atom % D).

Instrumentation and measurements: NMR spectra were recorded on a JEOL JNM-LA 400 FT-NMR or a Bruker Avance 400 or 200 NMR spectrometer. Chemical shifts are referenced to internal solvent resonances and are reported relative to tetramethylsilane (^1H NMR), 15% $\text{BF}_3\cdot\text{Et}_2\text{O}$ (^{11}B NMR), and 85% phosphoric acid (^{31}P NMR), respectively.^[88] IR spectra were obtained on a Shimadzu FTIR-8400s spectrometer. Elemental analyses were carried out with an Elementar vario EL or EL III instrument. Average molar masses (\bar{M}_n) and molar mass distributions (\bar{M}_w/\bar{M}_n) were determined by SEC in THF at 20°C (flow rate = 1.0 mL min⁻¹) on a Polymer Laboratories PL50 apparatus equipped with a refractive index detector and a PLgel 5 Å MIXED-C column. The polymer samples were dissolved in THF (2 mg mL⁻¹). The SEC traces of the polymers all exhibited a unimodal and symmetrical peak. The average molar mass values (\bar{M}_{SEC}) of the PCLs were calculated from the linear polystyrene calibration curve using the correction coefficient previously reported ($\bar{M}_{\text{SEC}} = \bar{M}_{\text{SECraw}} \times 0.56$).^[44] Monomer conversions were calculated from the integration (Int.) ratio (Int.P(CL)/[Int.P(CL) + Int.(CL)]) of the $\text{CH}_2\text{OC(O)}$ methylene triplet ($\delta = 4.04$ ppm) in the ^1H NMR spectrum of the crude polymer sample.

Synthesis of the bis(phosphinimino)methanide bis-borohydride complexes

[[CH(PPh₂NSiMe₃)₂]La(BH₄)₂(THF)] (1): THF (25 mL) was condensed at -78°C onto a mixture of [La(BH₄)₃(THF)₃] (600 mg, 1.50 mmol) and K[CH(PPh₂NSiMe₃)₂] (895 mg, 1.50 mmol) and the resulting reaction mixture was stirred for 16 h at 60°C. The colorless solution was filtered and the solvent evaporated in vacuo. Then toluene (10 mL) was condensed onto the residue. The mixture was heated carefully until the solution became clear. The solution was allowed to stand at ambient temperature to obtain the product as a colorless powder after 16 h. Yield: 842 mg, 1.10 mmol, 74%. Single crystals were obtained by crystallization from hot THF. ^1H NMR ([D₈]THF, 400 MHz, 25°C): $\delta = 0.22$ (s, 18H; SiMe₃), 1.02–1.64 (br, 8H; BH₄), 1.90 (ms, 4H; THF), 2.02 (t, $J_{\text{H,P}} = 2.1$ Hz, 1H; CH), 3.74 (ms, 4H; THF), 7.41–7.84 ppm (m, 20H; Ph); $^{13}\text{C}\{^1\text{H}\}$ NMR ([D₈]THF, 100.4 MHz, 25°C): $\delta = 4.3$ (SiMe₃), 16.6 (CH), 26.1 (THF), 67.9 (THF), 128.2–128.4 (m, *m*-Ph), 130.8 (*p*-Ph), 131.0–131.1 (m, *o*-Ph), 131.9–132.2 ppm (m, *i*-Ph); ^{31}P NMR ([D₈]THF, 101.3 MHz, 25°C): $\delta = 15.6$ ppm; ^{11}B NMR ([D₈]THF, 128.15 MHz, 25°C): $\delta = -22.4$ ppm (brqt, $J_{\text{H,B}} = 83$ Hz); IR: $\tilde{\nu} = 693$ (s), 832 (vs), 931 (m), 1072 (s), 1094 (s), 1131 (s), 1161 (w), 1254 (m), 1434 (m), 1976 (w), 2151 (m), 2210 (m), 2424 (w), 2949 (w), 3056 cm⁻¹ (w); MS (EI, 70 eV, 180°C): m/z (%): 712 (33) [$\text{M}-\text{CH}_3$]⁺, 698 (14) [CH(PPh₂NSiMe₃)₂La]⁺, 581 (25), 569 (97), 569 (97), 558 (84) [CH(PPh₂NSiMe₃)₂]⁺, 544 (100) [CH(PPh₂NSiMe₃)₂-CH₃]⁺, 493 (85), 481 (23), 455 (59), 394 (36), 348 (11) [$\text{M}-2\text{BH}_4$]⁺/2, 287 (26), 272 (48) [Ph₂PNSiMe₃]⁺, 183 (43), 135 (73), 121 (90), 73 (60) [SiMe₃]⁺, 43 (20); elemental analysis calcd (%) for C₃₅H₅₁B₂N₂O_{0.5}Si₂P₂La (1-0.5THF; 762.73): calcd. C 51.99, H 6.74, N 3.67; found: C 51.43, H 7.32, N 2.72.

[[CH(PPh₂NSiMe₃)₂]Y(BH₄)₂] (2): THF (25 mL) was condensed at -78°C onto a mixture of NaBH₄ (42 mg, 1.10 mmol) and in situ prepared [[CH(PPh₂NSiMe₃)₂]YCl₂]₂ (0.25 mmol) and the resulting colorless reaction mixture was stirred for 16 h at 60°C. The colorless solution was filtered and concentrated until a precipitate appeared. The mixture was heated carefully until the solution became clear. The solution was then allowed to stand at ambient temperature to obtain the product as colorless crystals after 6 h. Yield: 171 mg, 0.25 mmol, 51% (single crystals). ^1H NMR ([D₈]THF, 400 MHz, 25°C): $\delta = 0.19$ (s, 18H; SiMe₃), 1.70–2.10 (br, 8H; BH₄), 1.94 (t, 1H; CH), 6.63–6.95 (m, 8H; *m*-Ph), 7.13–7.18 (m, 8H; *o*-Ph), 7.79–7.84 ppm (m, 4H; *p*-Ph); $^{13}\text{C}\{^1\text{H}\}$ NMR ([D₈]THF, 100.4 MHz, 25°C): $\delta = 3.5$ (SiMe₃), 16.3 (CH), 128.1, 128.6 (2 t, *m*-Ph, $J_{\text{C,P}} = 6$ Hz, $J_{\text{H,P}} = 4.2$ Hz), 130.8 (*p*-Ph), 131.1 (t, $J_{\text{C,P}} = 5$ Hz, *o*-Ph), 131.7 (*p*-Ph), 132.1 (t, $J_{\text{C,P}} = 5$ Hz, *o*-Ph), 135.8 ppm (*i*-Ph); ^{31}P NMR ([D₈]THF, 101.3 MHz, 25°C): $\delta = 17.8$ ppm (d, $J_{\text{Y,P}} = 7.6$ Hz); ^{11}B NMR ([D₈]THF, 128.15 MHz, 25°C): $\delta = -24.7$ ppm (brqt, $J_{\text{H,B}} = 108$ Hz); IR: $\tilde{\nu} = 733$ (s), 841 (vs), 987 (m), 1094 (vs), 1192 (m), 1256 (w), 1437 (m), 1579 (w), 1971 (w), 2163 (s), 2216 (s), 2486 (m), 2943 (m), 3058 cm⁻¹ (w); MS (EI, 70 eV, 180°C): m/z (%): 736 (19), 721 (22), 676 (3) [M^+], 661 (100) [$\text{M}-\text{CH}_3$]⁺, 647 (39), 586 (100), 569 (99), 558 (14) [CH(PPh₂NSiMe₃)₂]⁺, 543 (97) [CH(PPh₂NSiMe₃)₂-CH₃]⁺, 493 (63), 358 (12), 323 (28)

[CH(PPh₂NSiMe₃)₂-CH₃]⁺, 272 (15) [Ph₂PNSiMe₃]⁺, 183 (18), 135 (27), 73 (33) [SiMe₃]⁺, 43 (16); elemental analysis calcd (%) for C₃₅H₄₇B₂N₂Si₂P₂Y (2; 676.37): C 55.05, H 7.00, N 4.14; found: C 55.54, H 7.28, N 3.42.

[[CH(PPh₂NSiMe₃)₂]Lu(BH₄)₂] (3): THF (25 mL) was condensed at -78°C onto a mixture of [Lu(BH₄)₃(THF)₃] (653 mg, 1.50 mmol) and K[CH(PPh₂NSiMe₃)₂] (895 mg, 1.50 mmol) and the resulting reaction mixture was stirred for 16 h at 60°C. The colorless solution was filtered and the solvent evaporated in vacuo. Then toluene (20 mL) was condensed onto the residue. The mixture was heated carefully until the solution became clear. The solution was layered with pentane and allowed to stand at ambient temperature to obtain the product as colorless crystals after 72 h. Yield: 822 mg, 0.94 mmol, 63%. ^1H NMR ([D₈]THF, 400 MHz, 25°C): $\delta = 0.35$ (s, 18H; SiMe₃), 1.45–2.08 (br, 8H; BH₄), 1.83 (t, $J_{\text{H,P}} = 3.8$ Hz, 1H; CH), 7.07–7.08 (m, 4H; Ph), 7.27–7.34 (m, 6H; Ph), 7.46–7.52 (m, 6H; Ph), 7.79–7.81 ppm (m, 4H; Ph); $^{13}\text{C}\{^1\text{H}\}$ NMR ([D₈]THF, 100.4 MHz, 25°C): $\delta = 3.3$ (SiMe₃), 17.6 (t, $J_{\text{C,P}} = 100$ Hz, CH), 128.6–128.9 (m, *m*-Ph), 130.5 (*p*-Ph), 131.5–131.7 (m, *o*-Ph), 132.2–132.4 ppm (m, *i*-Ph); ^{31}P NMR ([D₈]THF, 101.3 MHz, 25°C): $\delta = 20.9$ ppm; ^{11}B NMR ([D₈]THF, 128.15 MHz, 25°C): $\delta = -25.8$ ppm; IR: $\tilde{\nu} = 740$ (s), 776 (w), 827 (s), 996 (w), 1112 (s), 1164 (w), 1241 (m), 1436 (m), 1587 (w), 1983 (w), 2079 (m), 2225 (w), 2309 (m), 2420 (w), 2654 (w), 2862 (w), 2945 cm⁻¹ (w); MS (EI, 70 eV, 180°C): m/z (%): 762 (9) [M^+], 747 (90) [$\text{M}-\text{CH}_3$]⁺, 733 (36) [CH(PPh₂NSiMe₃)₂Lu]⁺, 672 (100), 657 (32), 569 (42), 558 (14) [CH(PPh₂NSiMe₃)₂]⁺, 543 (96) [CH(PPh₂NSiMe₃)₂-CH₃]⁺, 493 (23), 366 (23) [$\text{M}-2\text{BH}_4$]⁺/2, 359 (17) [(CH(PPh₂NSiMe₃)₂Lu-CH₃)]⁺/2, 272 (13) [Ph₂PNSiMe₃]⁺, 183 (10), 135 (18), 121 (19), 73 (21) [SiMe₃]⁺, 43 (10); elemental analysis calcd (%) for C₃₅H₅₁B₂N₂O_{0.5}Si₂P₂Lu (3+THF; 834.53): C 50.37, H 6.64, N 3.36; found: C 50.04, H 6.45, N 2.89.

X-ray crystallographic studies of 1–3: Crystals of 1–3 were grown from THF or toluene. Suitable crystals of compounds 1–3 were covered in mineral oil (Aldrich) and mounted on a glass fiber. The crystal was transferred directly into the stream of N₂ of a Stoe IPDS 2 or Stoe IPDS 2T diffractometer at -73 or -123°C. Subsequent computations were carried out on an Intel Pentium IV PC.

All structures were solved by the Patterson method (SHELXS-97^[89]). The remaining non-hydrogen atoms were located from successive difference Fourier map calculations. The refinements were carried out by using full-matrix least-squares techniques on F_o , minimizing the function $(F_o - F_c)^2$, with the weight defined as $4F_o^2/(F_o^2 + F_c^2)$ and F_o and F_c are the observed and calculated structure factor amplitudes using the program SHELXL-97.^[89] The positions of carbon-bound hydrogen atoms were calculated and allowed to ride on the carbon atoms to which they are bonded. The hydrogen atom contributions of compounds 1–3 were calculated but not refined. The locations of the largest peaks in the final difference Fourier map calculation as well as the magnitude of the residual electron densities in each case were of no chemical significance.

1·2THF: C₃₅H₅₃B₂LaN₂OP₂Si₂, monoclinic, $P2_1/n$ (No. 14), lattice constants $a = 10.0940(4)$, $b = 35.345(2)$, $c = 14.2018(6)$ Å, $\beta = 103.779(3)^\circ$, $V = 4921.0(4)$ Å³, $Z = 4$, $\mu(\text{Mo-K}\alpha) = 1.018$ mm⁻¹, $\theta_{\text{max}} = 25.02^\circ$, 8647 [$R_{\text{int}} = 0.0433$] independent reflections measured of which 7069 were considered observed with $I > 2\sigma(I)$, max. residual electron density = 1.219 and -0.809 e Å⁻³, 484 parameters, $R1$ ($I > 2\sigma(I)$) = 0.0408; $wR2$ (all data) = 0.1135.

2: C₃₁H₄₇B₂N₂P₂Si₂Y, monoclinic, $P2_1/n$ (No. 14), lattice constants $a = 9.7964(7)$, $b = 17.4944(8)$, $c = 21.4015(15)$ Å, $\beta = 91.599(6)^\circ$, $V = 3666.4(4)$ Å³, $Z = 4$, $\mu(\text{Mo-K}\alpha) = 1.765$ mm⁻¹, $\theta_{\text{max}} = 25.03^\circ$, 6440 [$R_{\text{int}} = 0.0614$] independent reflections measured of which 4890 were considered observed with $I > 2\sigma(I)$, max. residual electron density = 0.313 and -0.295 e Å⁻³, 399 parameters, $R1$ ($I > 2\sigma(I)$) = 0.0404, $wR2$ (all data) = 0.0793.

3: C₃₁H₄₇B₂N₂LuP₂Si₂, monoclinic, $P2_1/n$ (No. 14), lattice constants $a = 9.7538(6)$, $b = 17.4791(7)$, $c = 21.3528(13)$ Å, $\beta = 91.622(5)^\circ$, $V = 3638.9(3)$ Å³, $Z = 4$, $\mu(\text{Mo-K}\alpha) = 2.889$ mm⁻¹, $\theta_{\text{max}} = 25.03^\circ$, 6400 [$R_{\text{int}} = 0.0484$] independent reflections measured of which 5307 were considered observed with $I > 2\sigma(I)$, max. residual electron density = 0.623 and

-1.233 e Å^{-3} , 399 parameters, $R1$ ($I > 2\sigma(I)$) = 0.0271, $wR2$ (all data) = 0.0592.

CCDC-751614, -751616, and 751616 contain the supplementary crystallographic data for this paper. These data can be obtained free of charge from The Cambridge Crystallographic Data Centre via www.ccdc.cam.ac.uk/data_request/cif.

Typical procedure for the polymerization of ϵ -caprolactone: In a glove box, a Schlenk flask was charged with a toluene (0.4 mL) solution of initiator **2** (7.1 mg, 10.50 μmol). A toluene solution of CL (120.0 mg, 1.05 mmol, 100 equiv in 0.6 mL) was added. The mixture was then immediately stirred at 20 °C for the appropriate time (reaction times have not been systematically optimized). The reaction was quenched with an excess of acidic methanol (ca. 1 mL of a 1.2 M HCl solution in MeOH). The resulting mixture was concentrated under vacuum and the conversion determined by ^1H NMR analysis of the residue. This crude polymer was then dissolved in CH_2Cl_2 and purified by precipitation in cold methanol, filtration and drying under vacuum.

Computational details: Yttrium, phosphorus, and silicon were treated with a Stuttgart–Dresden pseudopotential in combination with their adapted basis set.^[90,91] The basis set was augmented by a set of polarization functions (d for phosphorus and silicon).^[92] Boron, carbon, and hydrogen atoms were described with a 6-31G(d,p) double- ζ basis set.^[93] Calculations were carried out at the DFT level of theory using the hybrid functional B3PW91.^[94,95] Geometry optimizations were carried out without any symmetry restrictions, the nature of the extrema (minimum) was verified with analytical frequency calculations. All these computations were performed with the Gaussian 03^[96] suite of programs. The electronic structure was studied by natural bond orbital (NBO) analysis.^[97]

Acknowledgements

This work was supported by the Deutsche Forschungsgemeinschaft (SPP 1166). We are grateful to the CNRS and UPS for financial support of this work. L.M. is grateful to Institut Universitaire de France, CalMip (CNRS, Toulouse, France) and CINES (CNRS, Montpellier, France) are acknowledged for use of their calculation facilities.

- [1] M. Vert, *Biomacromolecules* **2005**, *6*, 538–546.
- [2] L. S. Nair, C. T. Laurencin, *Prog. Polym. Sci.* **2007**, *32*, 762–798.
- [3] K. Sudesh, H. Abe, Y. Doi, *Prog. Polym. Sci.* **2000**, *25*, 1503–1555.
- [4] Y. Ikada, H. Tsuji, *Macromol. Rapid Commun.* **2000**, *21*, 117–132.
- [5] A.-C. Albertsson, I. K. Varma, *Biomacromolecules* **2003**, *4*, 1466–1486.
- [6] K. M. Stridsberg, M. Ryner, A.-C. Albertsson, *Adv. Polym. Sci.* **2002**, *157*, 42–65.
- [7] A.-C. Albertsson, I. K. Varma, *Biomacromolecules* **2002**, *3*, 1–41.
- [8] G. Rokicki, *Prog. Polym. Sci.* **2000**, *25*, 259–342.
- [9] A. P. Dove, *Chem. Commun.* **2008**, 6446–6470.
- [10] H. Yasuda, *J. Organomet. Chem.* **2002**, *647*, 128–138.
- [11] Z. Hou and Y. Wakatsuki, *Coord. Chem. Rev.* **2002**, *231*, 1–22.
- [12] H. Yasuda, *Prog. Polym. Sci.* **2000**, *25*, 573–626.
- [13] S. Agarwal, C. Mast, K. Denicke, A. Greiner, *Macromol. Rapid Commun.* **2000**, *21*, 195–212.
- [14] M. Le Hellaye, N. Fortin, J. Guilloteau, A. Soum, S. Lecommandoux, S. M. Guillaume, *Biomacromolecules* **2008**, *9*, 1924–1933.
- [15] M. Helou, O. Misericordie, J.-M. Brusson, J.-F. Carpentier, S. M. Guillaume, *Chem. Eur. J.* **2008**, *14*, 8772–8775.
- [16] M. Helou, O. Misericordie, J.-M. Brusson, J.-F. Carpentier, S. M. Guillaume, *Adv. Synth. Catal.* **2009**, *351*, 1312–1324.
- [17] L. R. Rieth, D. R. Moore, E. Lobkovsky, G. W. Coates, *J. Am. Chem. Soc.* **2002**, *124*, 15239–15248.
- [18] J. Wu, T.-L. Yu, C.-T. Chen, C.-C. Lin, *Coord. Chem. Rev.* **2006**, *250*, 602–626.
- [19] B. J. O'Keefe, M. A. Hillmyer, W. B. Tolman, *J. Chem. Soc. Dalton Trans.* **2001**, 2215–2224.
- [20] W. Kuran, *Prog. Polym. Sci.* **1998**, *23*, 919–992.
- [21] E. Zange, *Chem. Ber.* **1960**, *93*, 652–657.
- [22] U. Mirsaidov, G. N. Boiko, A. Kurbonbekov, A. Rakhimova, *Dokl. Akad. Nauk Tadzh. SSR* **1986**, *29*, 608–611.
- [23] U. Mirsaidov, A. Kurbonbekov, *Dokl. Akad. Nauk Tadzh. SSR* **1985**, *28*, 219–220.
- [24] U. Mirsaidov, I. B. Shaimuradov, M. Khikmatov, *Zh. Neorg. Khim.* **1986**, *31*, 1321–1323.
- [25] S. M. Cendrowski-Guillaume, G. Le Gland, M. Nierlich, M. Ephritikhine, *Organometallics* **2000**, *19*, 5654–5660.
- [26] S. M. Cendrowski-Guillaume, M. Nierlich, M. Lance, M. Ephritikhine, *Organometallics* **1998**, *17*, 786–788.
- [27] D. Barbier-Baudry, O. Blacque, A. Hafid, A. Nyassi, H. Sitzmann, M. Visseaux, *Eur. J. Inorg. Chem.* **2000**, 2333–2336.
- [28] S. M. Cendrowski-Guillaume, G. Le Gland, M. Lance, M. Nierlich, M. Ephritikhine, *C. R. Chim.* **2002**, *5*, 73–80.
- [29] Z. Hou, Y. Wakatsuki, *J. Organomet. Chem.* **2002**, *647*, 61–70.
- [30] J. Thuilliez, R. Spitz, C. Boisson, *Macromol. Chem. Phys.* **2006**, *207*, 1727–1731.
- [31] M. Visseaux, T. Chenal, P. Roussel, A. Mortreux, *J. Organomet. Chem.* **2006**, *691*, 86–92.
- [32] F. Bonnet, M. Visseaux, D. Barbier-Baudry, E. Vigier, M. M. Kubicki, *Chem. Eur. J.* **2004**, *10*, 2428–2434.
- [33] M. Terrier, M. Visseaux, T. Chenal, A. Mortreux, *J. Polym. Sci. Part A* **2007**, *45*, 2400–2409.
- [34] M. Visseaux, M. Mainil, M. Terrier, A. Mortreux, P. Roussel, T. Mathivet, M. Destarac, *Dalton Trans.* **2008**, 4558–4561.
- [35] F. Bonnet, C. D. C. Violante, P. Roussel, A. Mortreux, M. Visseaux, *Chem. Commun.* **2009**, 3380–3382.
- [36] P. Zinck, A. Valente, A. Mortreux, M. Visseaux, *Polymer* **2007**, *48*, 4609–4614.
- [37] F. Bonnet, A. R. Cowley, P. Mountford, *Inorg. Chem.* **2005**, *44*, 9046–9055.
- [38] Y. Nakayama, K. Sasaki, N. Watanabe, Z. Cai, T. Shiono, *Polymer* **2009**, *50*, 4788–4793.
- [39] Y. Nakayama, S. Okuda, H. Yasuda, T. Shiono, *React. Funct. Polym.* **2007**, *67*, 798–806.
- [40] T. V. Mahrova, G. K. Fukin, A. V. Cherkasov, A. A. Trifonov, N. Ajellal, J.-F. Carpentier, *Inorg. Chem.* **2009**, *48*, 4258–4266.
- [41] G. G. Skvortsov, M. V. Yakovenko, P. M. Castro, G. K. Fukin, A. V. Cherkasov, J.-F. Carpentier, A. A. Trifonov, *Eur. J. Inorg. Chem.* **2007**, 3260–3267.
- [42] N. Ajellal, D. M. Lyubov, M. A. Sinenko, G. K. Fukin, A. V. Cherkasov, C. M. Thomas, J.-F. Carpentier, A. A. Trifonov, *Chem. Eur. J.* **2008**, *14*, 5440–5448.
- [43] N. Barros, P. Mountford, S. M. Guillaume, L. Maron, *Chem. Eur. J.* **2008**, *14*, 5507–5518.
- [44] S. M. Guillaume, M. Schappacher, A. Soum, *Macromolecules* **2003**, *36*, 54–60.
- [45] I. Palard, A. Soum, S. M. Guillaume, *Macromolecules* **2005**, *38*, 6888–6894.
- [46] I. Palard, A. Soum, S. M. Guillaume, *Chem. Eur. J.* **2004**, *10*, 4054–4062.
- [47] I. Palard, M. Schappacher, A. Soum, S. M. Guillaume, *Polym. Int.* **2006**, *55*, 1132–1137.
- [48] S. M. Guillaume, M. Schappacher, N. M. Scott, R. Kempe, *J. Polym. Sci. Part A. J. Polym. Sci. Part A* **2007**, *45*, 3611–3619.
- [49] D. M. Lyubov, A. M. Bubnov, G. K. Fukin, F. M. Dolgushin, M. Y. Antipin, O. Pelcé, M. Schappacher, S. M. Guillaume, A. A. Trifonov, *Eur. J. Inorg. Chem.* **2008**, 2090–2098.
- [50] G. Wu, W. Sun, Z. Shen, *React. Funct. Polym.* **2008**, *68*, 822–830.
- [51] M. T. Gamer, P. W. Roesky, I. Palard, M. Le Hellaye, S. M. Guillaume, *Organometallics* **2007**, *26*, 651–657.
- [52] I. Palard, M. Schappacher, B. Belloncle, A. Soum, S. M. Guillaume, *Chem. Eur. J.* **2007**, *13*, 1511–1521.
- [53] N. Barros, M. Schappacher, P. Dessuge, L. Maron, S. M. Guillaume, *Chem. Eur. J.* **2008**, *14*, 1881–1890.

- [54] a) M. Schappacher, N. Fur, S. M. Guillaume, *Macromolecules* **2007**, *40*, 8887–8896; b) M. Schappacher, A. Soum, S. M. Guillaume, *Biomacromolecules* **2006**, *7*, 1373–1379.
- [55] G. G. Skvortsov, M. V. Yakovenko, G. K. Fukin, A. V. Cherkasov, A. A. Trifonov, *Russ. Chem. Bull.* **2007**, *56*, 1742–1748.
- [56] F. Yuan, Y. Zhu, L. Xiong, *J. Organomet. Chem.* **2006**, *691*, 3377–3382.
- [57] D. Barbier-Baudry, F. Bouyer, A. S. M. Bruno, M. Visseaux, *Appl. Organomet. Chem.* **2006**, *20*, 24–31.
- [58] F. Yuan, J. Yang, L. Xiong, *J. Organomet. Chem.* **2006**, *691*, 2534–2539.
- [59] Z. Xu, Z. Lin, *Coord. Chem. Rev.* **1996**, *156*, 139–162.
- [60] V. D. Makhaev, *Russ. Chem. Commun.* **2000**, *69*, 727–746.
- [61] M. Ephritikhine, *Chem. Rev.* **1997**, *97*, 2193–2242.
- [62] T. J. Marks, J. R. Kolb, *Chem. Rev.* **1977**, *77*, 263–293.
- [63] R. G. Cavell, R. P. K. Babu, K. Aparna, *J. Organomet. Chem.* **2001**, *617–618*, 158–169.
- [64] R. G. Cavell, *Curr. Sci.* **2000**, *78*, 440–451.
- [65] N. D. Jones, R. G. Cavell, *J. Organomet. Chem.* **2005**, *690*, 5485–5496.
- [66] T. K. Panda, P. W. Roesky, *Chem. Soc. Rev.* **2009**, *38*, 2782–2804.
- [67] M. T. Gamer, S. Dehnen, P. W. Roesky, *Organometallics* **2001**, *20*, 4230–4236.
- [68] M. T. Gamer, M. Rastaetter, P. W. Roesky, A. Steffens, M. Glanz, *Chem. Eur. J.* **2005**, *11*, 3165–3172.
- [69] M. T. Gamer, P. W. Roesky, *J. Organomet. Chem.* **2002**, *647*, 123–127.
- [70] T. K. Panda, P. Benndorf, P. W. Roesky, *Z. Anorg. Allg. Chem.* **2005**, *631*, 81–84.
- [71] T. K. Panda, M. T. Gamer, P. W. Roesky, *Inorg. Chem.* **2006**, *45*, 910–916.
- [72] T. K. Panda, A. Zulys, M. T. Gamer, P. W. Roesky, *Organometallics* **2005**, *24*, 2197–2202.
- [73] M. Rastätter, A. Zulys, P. W. Roesky, *Chem. Commun.* **2006**, 874–876.
- [74] M. Rastätter, A. Zulys, P. W. Roesky, *Chem. Eur. J.* **2007**, *13*, 3606–3616.
- [75] A. Zulys, T. K. Panda, M. T. Gamer, P. W. Roesky, *Chem. Commun.* **2004**, 2584–2585.
- [76] R. Appel, I. Ruppert, *Z. Anorg. Allg. Chem.* **1974**, *406*, 131–144.
- [77] Y. Yamashita, E. Takemoto, E. Ihara, H. Yasuda, *Macromolecules* **1996**, *29*, 1798–1806.
- [78] H. Yasuda, E. Ihara, *Bull. Chem. Soc. Jpn.* **1997**, *70*, 1745–1767.
- [79] M. T. Gamer, P. W. Roesky, *Z. Anorg. Allg. Chem.* **2001**, *627*, 877–881.
- [80] The bonding situation in the drawings of the ligand system in all schemes is simplified for clarity.
- [81] F. T. Edelmann, D. M. M. Freckmann, H. Schumann, *Chem. Rev.* **2002**, *102*, 1851–1896.
- [82] P. W. Roesky, *Z. Anorg. Allg. Chem.* **2006**, *632*, 1918–1926.
- [83] M. Wiecko, S. Marks, T. K. Panda, P. W. Roesky, *Z. Anorg. Allg. Chem.* **2009**, *635*, 931–935.
- [84] S. Penczek, T. Biela, A. Duda, *Macromol. Rapid Commun.* **2000**, *21*, 941–950.
- [85] S. Penczek, M. Cypriak, A. Duda, P. Kubisa, S. Slomkowski, *Prog. Polym. Sci.* **2007**, *32*, 247–282.
- [86] N. Meyer, J. Jenter, P. W. Roesky, G. Eickerling, W. Scherer, *Chem. Commun.* **2009**, 4693–4695.
- [87] M. D. Taylor, C. P. Carter, *J. Inorg. Nucl. Chem.* **1962**, *24*, 387–391.
- [88] S. Berger, U. Zeller, *Angew. Chem.* **2004**, *116*, 2070–2083.
- [89] G. M. Sheldrick, *Acta Crystallogr. Sect. A* **2008**, *64*, 112–122.
- [90] A. Bergner, M. Dolg, W. Küchle, H. Stoll, H. Preuss, *Mol. Phys.* **1993**, *80*, 1431–1441.
- [91] D. Andrae, U. Häussermann, M. Dolg, H. Stoll, H. Preuss, *Theor. Chim. Acta* **1990**, *77*, 123.
- [92] A. W. Ehlers, M. Böhme, S. Dapprich, A. Gobbi, A. Höllwarth, V. Jonas, K. F. Köhler, R. Stegmann, A. Veldkamp, G. Frenking, *Chem. Phys. Lett.* **1993**, *208*, 111–114.
- [93] P. C. Hariharan, J. A. Pople, *Theor. Chim. Acta* **1973**, *28*, 213–222.
- [94] A. D. Becke, *J. Chem. Phys.* **1993**, *98*, 5648–5652.
- [95] K. Burke, J. P. Perdew, W. Yang in *Electronic Density Functional Theory: Recent Progress and New Directions* (Eds.: J. F. Dobson, G. Vignale, M. P. Das), Springer, Heidelberg, **1998**.
- [96] Gaussian 03, Revision E.01, M. J. Frisch, G. W. Trucks, H. B. Schlegel, G. E. Scuseria, M. A. Robb, J. R. Cheeseman, V. G. Zakrzewski, J. A. Montgomery, Jr., R. E. Stratman, J. C. Burant, S. Dapprich, J. M. Millam, A. D. Daniels, K. N. Kudin, M. C. Strain, O. Farkas, J. Tomasi, V. Barone, M. Cossi, R. Cammi, B. Mennucci, C. Pomelli, C. Adamo, S. Clifford, J. Ochterski, G. A. Petersson, P. Y. Ayala, Q. Cui, K. Morokuma, D. K. Malick, A. D. Rabuck, K. Raghavachari, J. B. Foresman, J. Cioslowski, J. V. Ortiz, A. G. Baboul, B. B. Stefanov, G. Liu, A. Liashenko, P. Piskorz, I. Komaromi, R. Gomperts, R. Martin, D. J. Fox, T. Keith, M. A. Al-Laham, C. Y. Peng, A. Nanayakkara, C. Gonzalez, M. Challacombe, P. M. W. Gill, B. Johnson, W. Chen, M. W. J. Wong, L. Andres, M. Head-Gordon, E. S. Replogle, J. A. Pople, Pittsburgh PA **2006**.
- [97] A. E. Reed, L. A. Curtiss, F. Weinhold, *Chem. Rev.* **1988**, *88*, 899–926.

Received: November 12, 2009
Published online: March 15, 2010